



ELSEVIER

Available online at [www.sciencedirect.com](http://www.sciencedirect.com)

ScienceDirect

journal homepage: [www.elsevier.com/locate/he](http://www.elsevier.com/locate/he)

## On the applicability of PdAg membranes in propane dehydrogenation processes

W.J.R. Ververs<sup>a</sup>, A. Arratibel Plazaola<sup>b</sup>, L. Di Felice<sup>a</sup>, F. Gallucci<sup>a,c,\*</sup>

<sup>a</sup> Inorganic Membranes and Membrane Reactors, Sustainable Process Engineering, Department of Chemical Engineering and Chemistry, Eindhoven University of Technology, P.O. Box 513, 5600 MB Eindhoven, the Netherlands

<sup>b</sup> TECNALIA, Basque Research and Technology Alliance (BRTA), Mikeletegi Pasealekua 2, 20009 Donostia-San Sebastian, Spain

<sup>c</sup> Eindhoven Institute for Renewable Energy Systems (EIRES), Eindhoven University of Technology, P.O. Box 513, 5600 MB Eindhoven, the Netherlands

### HIGHLIGHTS

- 2 double-skin PdAg membranes were tested in emulated PDH conditions.
- 2 different configurations of membrane integration were compared.
- At lower temperatures, membrane activity is improved in the PDH process.
- Cascade integration allows for an improved membrane performance and lifetime.

### ARTICLE INFO

#### Article history:

Received 15 February 2023

Received in revised form

12 June 2023

Accepted 16 June 2023

Available online xxx

#### Keywords:

Membranes

Propane dehydrogenation

Membrane reactors

Membrane stability

### ABSTRACT

The applicability of PdAg membranes in the propane dehydrogenation process has been evaluated in this work. The integration of membranes into the propane dehydrogenation process has the potential of making a significant step forward in energy and resource efficiency of the selective production of propylene. To assess the compatibility of the PdAg membrane with the process conditions of propane dehydrogenation, two double-skin PdAg membranes were exposed to the emulated process conditions of two cases: 1. A fully integrated membrane-reactor system (higher temperature) and 2. A cascade of catalyst and membrane separator units (lower temperature). The results of this study showed that at high temperature (475–500 °C) strong reduction of the hydrogen flux is observed during exposure to reactant and product containing mixtures. The reason for this is the deposition of carbonaceous species on the active sites of the membrane. Additionally, also the lifetime of the membrane (in terms of selectivity) was significantly lower due to the regeneration performed at high temperature in diluted air. The lower temperature experiments (300–350 °C) showed a much lower degree of deactivation and at the same time the membrane could be regenerated in air repeatedly without visible reduction of its selectivity. These findings show that the DS-PdAg membrane can be repeatedly exposed to reaction-regeneration cycles at acceptable activity and without significant loss of selectivity when operated in a cascade configuration at a temperature at or below 350 °C.

© 2023 The Authors. Published by Elsevier Ltd on behalf of Hydrogen Energy Publications LLC. This is an open access article under the CC BY license (<http://creativecommons.org/licenses/by/4.0/>).

\* Corresponding author.

E-mail address: [f.gallucci@tue.nl](mailto:f.gallucci@tue.nl) (F. Gallucci).

<https://doi.org/10.1016/j.ijhydene.2023.06.202>

0360-3199/© 2023 The Authors. Published by Elsevier Ltd on behalf of Hydrogen Energy Publications LLC. This is an open access article under the CC BY license (<http://creativecommons.org/licenses/by/4.0/>).

## Introduction

Propylene is a chemical building block that has been in high demand already for many years, this demand is expected to keep on growing in the near future [1–3]. Most of the propylene is being used as a starting material to produce multiple different polymers (polypropylene, polyethylene, polyethylene terephthalate etc.). Currently cracking processes like fluid catalytic cracking and steam cracking are the major sources of propylene. However, for these processes, propylene is a side-product, therefore they are not suitable of fulfilling the increasing demand that is expected to continue growing for the coming years [4]. Besides the forecasted supply-demand mismatch, sustainable processes generating chemical building blocks are also much desired. The development of a process that can selectively produce propylene in an energy and resource efficient way could become very important in the highly needed circular economy. Since this circular economy will most likely involve breaking down materials to rebuild new products, a process making a direct and efficient connection from propane to propylene could become an important link in this system. An already existing way of selectively producing propylene is dehydrogenation of propane, with the CATOFIN and OLEFLEX processes being the currently most important commercial ways of performing propane dehydrogenation. The advantages of these two processes are that they are large scale proven with commercially interesting product yields. However, they are operated at very high temperatures (i.e. 550–650 °C) resulting in a high energy consumption and high amount of coke formation, with accompanied periodic regeneration of the catalyst required [5].

To make propane dehydrogenation more sustainable, the resource efficiency needs to be improved and/or the energy consumption reduced. Both these aspects could possibly be achieved with the integration of membranes in the process. For example, by removing the H<sub>2</sub> from the propane dehydrogenation reaction, the thermodynamically limited conversion can be overcome, potentially leading to higher propylene yield following the Le Chatelier's principle. This has already been shown experimentally by multiple works [6–10]. On the other hand, this principle also allows to decrease the reaction temperature while remaining at an acceptable conversion. A lower temperature will lead to a reduced energy consumption and a reduction of by-products and in particular reduced coke formation and thus longer lifetime of the catalysts.

Several different membrane types have already been suggested and tested for their integration in the propane dehydrogenation process. The most abundant are Pd-based, zeolite and ceramic type membranes. Dangwal et al. successfully implemented an alumina supported silicalite membrane together with a Pt/Al<sub>2</sub>O<sub>3</sub> catalyst. The integration of the silicalite membrane led to an improved propylene yield of 47% at 600 °C and 5 atm [11]. The advantage of using a ceramic membrane is that it can be operated at high temperature, meaning that the process can be operated at a temperature ideal for the currently available PDH catalysts. Kim et al. showed that also SAPO-34 zeolite membranes can provide enhanced propylene yield to a packed bed reactor system with a Na<sub>2</sub>O–Cr<sub>2</sub>O<sub>3</sub>/Al<sub>2</sub>O<sub>3</sub> catalyst. Propylene yield was improved

from 37% to 59% upon the addition of the SAPO-34 zeolite membrane [7]. Pd-based membranes have generally better selectivity-permeance properties compared to zeolite and ceramic membranes [12]. However, Pd-based membranes are expected to be significantly more expensive than the alternatives, which is a techno-economical threshold that needs to be overcome, by taking advantage of the superior permeation properties. Multiple works have already attempted direct integration of Pd-based membranes into catalytic packed bed propane dehydrogenation systems. Quicker et al. achieved an improvement of propylene yield from 22% to 26% by the addition of a supported Pd membrane to a packed bed reactor of commercial propane dehydrogenation catalyst [13]. Similar studies using Pd-based membranes include Collins et al. gaining a yield improvement of 29.6%–39.6% and Sheintuch et al. obtaining a propylene yield of 70 [8,14]. The use of Pd-based membranes requires the operation at lower temperatures compared to zeolite and ceramic membranes. This is a disadvantage from a process performance point of view, but an advantage when looking at energy efficiency. Additionally, most works applying Pd-based membranes in combination with propane and propylene report a flux reduction caused by co-adsorption and coke formation [8,13,15–20].

In the last few of years, large improvements have been made in the optimization of Pd-based membranes. Currently, membranes can be produced with H<sub>2</sub> permeances of 5 10<sup>-6</sup> mol s<sup>-1</sup> m<sup>-2</sup> Pa<sup>-1</sup> and H<sub>2</sub>/N<sub>2</sub> perm-selectivity well above 25,000 [21–23]. Due to these developments, research into the integration of Pd-based membranes in propane dehydrogenation processes is continued today.

A major topic in this research is the design of the (integrated) membrane reactor system. Commonly proposed configurations can be referred to as integrated membrane reactor architecture and the cascade of conventional reactors and membrane separation units (referred to by some authors as open architecture), shown in Fig. 1 [24]. In the case of integrated membrane reactor, the membranes and the catalyst are placed in the same unit, leading to a compact design [25]. The key enabler of this configuration is that operating conditions must be matching for the membranes and the catalyst, allowing that both the membrane and the catalyst can be operated in optimal conditions. This is an important requirement for a system in which the building blocks and reaction are strongly temperature dependent. The H<sub>2</sub> flux for Pd-based membranes increases with temperature but its mechanical stability is bound to a range of roughly 300–525 °C. Below 300 °C the risk of hydrogen embrittlement becomes significant, especially in combination with a strongly endothermic process that makes it difficult to mitigate temperature gradients in the system, increasing the risk of local cold spots. Above 525 °C the expected lifetime of the membranes and their sealings will be reduced [26]. When we look at the catalyst, a higher activity is observed at higher temperatures. Besides the membrane and the catalyst, the propane dehydrogenation reaction is also highly temperature dependent. Higher temperatures favour higher conversion, faster kinetics, but lower selectivity. The final and for sure not least important temperature dependency of the system is deactivation of catalyst and membrane. The higher the temperature, the faster is their deactivation. Summarizing all the above

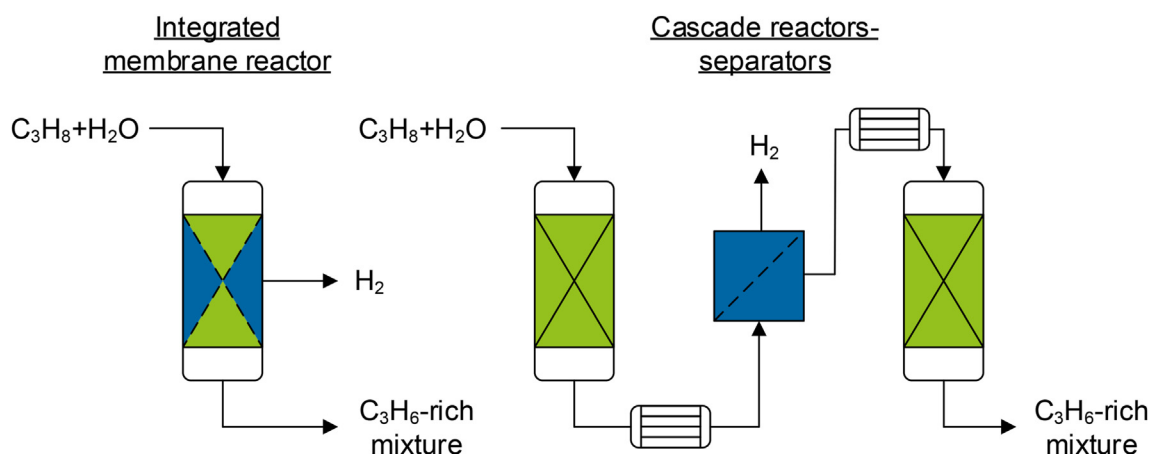


**Fig. 1 – Illustration of integrated membrane reactor and cascade reactor-separator configuration membrane reactors for propane dehydrogenation.**

temperature effects, it can be stated that a complete integration of Pd-based membranes requires highly complex operation.

A commonly proposed alternative to the fully integrated membrane design is the cascade of reactors and membrane separators. In this case, the membrane and the catalyst are placed in separate units, often one or multiple combinations of reactor-separator in series [6,15]. This configuration allows the decoupling of the reaction and separation temperatures, such that catalyst can be operated at maximum activity and critical membrane deactivation can be reduced. Both Ricca et al. and Peters et al. already showed that Pd-based membranes have a much better performance at temperatures below 400 °C when exposed to propane and propylene [6,15].

In this work, the applicability of Pd-based membranes in both the integrated membrane reactor and the cascade configuration of reactor(s)/separator(s) is evaluated. The focus is on the performance in PDH conditions and regenerability. The conditions in the integrated membrane reactor were emulated at 475–500 °C, the cascade configuration at 300–400 °C. For this work, double-skin (DS) PdAg membranes have been used since they are the cutting-edge technology in the area of Pd-based membranes, close to commercial implementation in membrane reactor technology [27]. Advantages of these membranes are their high permeance, high selectivity, improved chemical and mechanical stability compared to conventional Pd-based membranes due to their added protective layer. Two of these DS-PdAg membranes were used for permeation and regeneration tests under relevant (emulated) PDH conditions. First the  $H_2$  separation performance in contact with propane dehydrogenation mixtures was tested and then the conditions of regeneration procedure were investigated.

## Experimental

### Membranes

The membranes used in this work were two identical (M1 and M2) tubular membranes produced according to the procedure

described in the work by Arratibel et al. [21]. The membranes are supported by asymmetric  $Al_2O_3$  supports provided by Rauschert Kloster Veilsdorf. The supports have a pore size of 100 nm at the external surface and a 14/7 mm OD/ID ratio. The supports were first treated with a simultaneous deposition of a PdAg layer via electroless plating after activation of the support with Pd seeds. The membranes were then annealed at 550 °C in a reducing atmosphere. Finally, the protective layer of 50 wt% YSZ and 50 wt%  $\gamma-Al_2O_3$  was deposited on top of the selective layer by dip-coating, followed by a calcination at 550 °C. The estimated thicknesses of the selective and protective layers are about 4–5 and 1  $\mu m$ . The membranes were sealed using Swagelok connectors with graphite ferules. After this procedure, the membranes were checked for possible defects, but the observed  $N_2$  permeance of both membranes was below  $1.13 \cdot 10^{-11} \text{ mol s}^{-1} \text{ m}^{-2} \text{ Pa}^{-1}$  (at  $\Delta p = 4 \text{ bar}$  and 20 °C).

Before starting the experiments, the membranes were activated by exposure to air at 400 °C for 2 min, after which the membrane flux was stabilized in  $H_2$ . The details and main performance indicators of the membranes after activation and stabilization can be found in Table 1. Selectivity values are given as minimum values since the  $N_2$  permeation flow was below the limit of the flow measurement equipment (0.2 mln  $\text{min}^{-1}$ ).

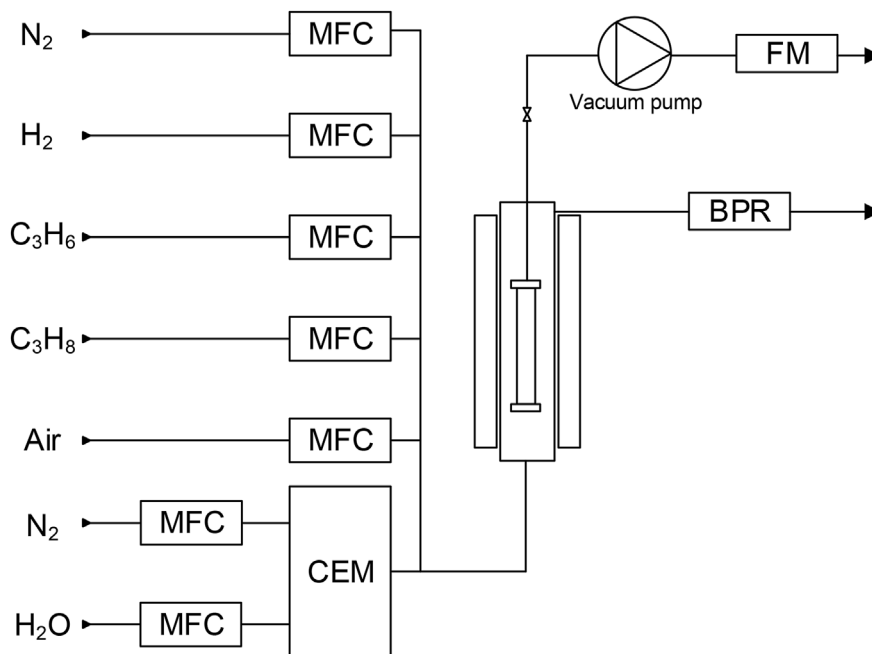
### Membrane tests

The membranes were tested in a membrane permeation setup, where temperature, pressure and gas feed flow rates and compositions can be controlled (Fig. 2). The feed flow rates were controlled using Brooks® Instrument mass flow controllers. Retentate pressure and steam generation are controlled by a back pressure regulator and a controlled-evaporator-mixer respectively, provided by Bronkhorst®. To analyse the membrane permeation behaviour, the permeate flow rate was measured using HORIBA-STECH bubble flow meters. The membrane module was heated using an electric heater. Temperatures were monitored using thermocouples at three different points inside the module. Pressure was monitored using pressure transmitters at the inlet and outlet

**Table 1 – Properties of membranes used in this work.**

Membrane	Type	Support	H <sub>2</sub> flux <sup>a</sup> (mol s <sup>-1</sup> m <sup>-2</sup> )	S <sub>H<sub>2</sub>/N<sub>2</sub></sub> <sup>b</sup>
M1	YSZ/Al <sub>2</sub> O <sub>3</sub> -PdAg	Tubular 14/7 Al <sub>2</sub> O <sub>3</sub>	0.390	>23,790
M2	YSZ/Al <sub>2</sub> O <sub>3</sub> -PdAg	Tubular 14/7 Al <sub>2</sub> O <sub>3</sub>	0.362	>22,100

<sup>a</sup> Measured in pure H<sub>2</sub> at 400 °C and 2 bar pressure difference.  
<sup>b</sup> Ratio of fluxes in pure H<sub>2</sub> and N<sub>2</sub> measured at 400 °C and 2 bar pressure difference.

**Fig. 2 – Schematic of the equipment used for membrane tests.**

of the module. To reduce the permeate pressure below atmospheric pressure a vacuum pump provided by Vacuum-brand® was used.

Two different gas mixtures were used for the experiments in this work. The compositions of the mixtures were selected to represent a gas mixture typical for the integrated and the cascade architectures in a vessel without catalyst. The compositions were based on a partially converted propane/steam (80/20) feed mixture. For integrated configuration, typical conversion values reported in literature are in the range of 30–50%, so in this work 40% was used as a reference value [7,8,11,13]. However, in a fully integrated membrane reactor the membrane is exposed to the gas mixture in the entire range of conversion (from inlet to outlet). An average gas mixture in contact with the membrane was emulated by taking half of the complete conversion of the unit (20%). For the cascade configuration, the gas mixture in contact with the membrane is equal to the gas mixture exiting the first catalytic reactor. For this a conversion of 14% is selected. The exact gas compositions adopted for the two cases can be found in Table 2.

Each experiment was composed of two parts: a permeation test in which also deactivation may occur (called hereafter permeation step) and a regeneration test. During the permeation step, either one of the PDH mixtures was fed to the

**Table 2 – Feed conditions used in the experimental tests during permeation step.**

	Integrated configuration	Cascade configuration
H <sub>2</sub>	13.1%	9.6%
C <sub>3</sub> H <sub>6</sub>	13.1%	9.8%
C <sub>3</sub> H <sub>8</sub>	52.5%	58.7%
H <sub>2</sub> O	16.4%	17.1%
N <sub>2</sub>	4.8%	4.8%
Retentate pressure	5 bar(a)	5 bar(a)
Permeate pressure	0.01 bar(a)	0.01 bar(a)
Temperature	475–500 °C	300–400 °C

membrane module at a selected temperature. The permeate flow rate was measured regularly (approximately every 10–20 min) to observe how the H<sub>2</sub> flux changes over time. After this permeation test, the membrane activity was significantly lowered, and regeneration was required. Reactive gasses were removed from the module by flushing nitrogen, after which a regeneration was performed by exposing the membrane for a fixed set amount of time (0.5–20 min) to a mixture of air and N<sub>2</sub>. Details of the regeneration steps are reported in the results and discussion. The regeneration step was always performed at the same temperature as the permeation step. To evaluate if the membrane was

completely regenerated, the flux in pure H<sub>2</sub> was measured and compared to the flux before the permeation-regeneration cycle. In case the flux was not completely recovered, an additional regeneration step was performed.

## Results and discussion

### Comparison of integrated and cascade configurations (M1)

First, the tests with membrane M1 were focussed on the separation behaviour in PDH conditions. Details of all these tests can be found in Tables 2 and 3. The membrane was first exposed to the cascade configuration conditions at 350-375-400 °C. First the results of the permeation steps will be analysed, afterwards, the results of the regeneration steps will be discussed. The experiment indicated with cycle 1 was not included in the analysis since a measurement failure made the obtained permeation data unreliable. However, it was included since it is relevant for the evaluation of the state of the membrane. The duration of the different permeation steps was not kept constant since the experiments were carried out to evaluate the effect of temperature on the rate of deactivation, so duration of the steps was not a critical parameter.

In Fig. 3a, H<sub>2</sub> flux over time is reported for the membrane exposed to the cascade configuration conditions at different

temperatures. For each temperature, a significant decrease of H<sub>2</sub> flux can be observed during the first 8 h of exposure to the mixture; after this, the H<sub>2</sub> flux seems to stabilize between 0.005 and 0.010 mol s<sup>-1</sup> m<sup>-2</sup>. Multiple works already reported a steep decrease of H<sub>2</sub> flux during exposure of Pd-based membranes to propylene containing mixtures [16,18–20]. The higher the temperature the more severe the reported deactivation (or flux decrease). This deactivation has been attributed to a propylene decomposition reaction that gradually covers all the active sites for the dissociative H<sub>2</sub> adsorption step of the permeation mechanism [15,28]. Besides the transient deactivation, dilution, external mass transfer limitations and adsorption of propane are expected to lower the permeated H<sub>2</sub>, however these phenomena are not expected to show transient behaviour over the timespan of multiple hours [29].

After exposing M1 to cascade configuration conditions, it was also exposed to integrated configuration conditions. In Fig. 3b, the H<sub>2</sub> flux over time in integrated configuration conditions is shown for the cases at 475 °C and 500 °C. A much steeper decrease of H<sub>2</sub> flux is observed where the deactivation takes place just in the first hour of exposure. After this initial decrease a stable H<sub>2</sub> flux is observed again. This behaviour can as well be attributed to deposition of carbonaceous species on the PdAg layer by propylene decomposition at high temperature. The complete set of permeation curves shows a strong correlation between temperature and deactivation rate

**Table 3 – Specifications of each permeation-regeneration cycle performed with M1.**

Experiment	Temperature	Configuration	Duration permeation step	Duration regeneration step
cycle 1	390 °C	Cascade	5.75 h	15 min
cycle 2	400 °C	Cascade	10.5 h	10 min +3 min
cycle 3	375 °C	Cascade	8.15 h	15 min
cycle 4	350 °C	Cascade	8.22 h	15 min
cycle 5	475 °C	Integrated	9.25 h	15 min +5 min
cycle 6	500 °C	Integrated	3.22 h	15 min +7.5 min

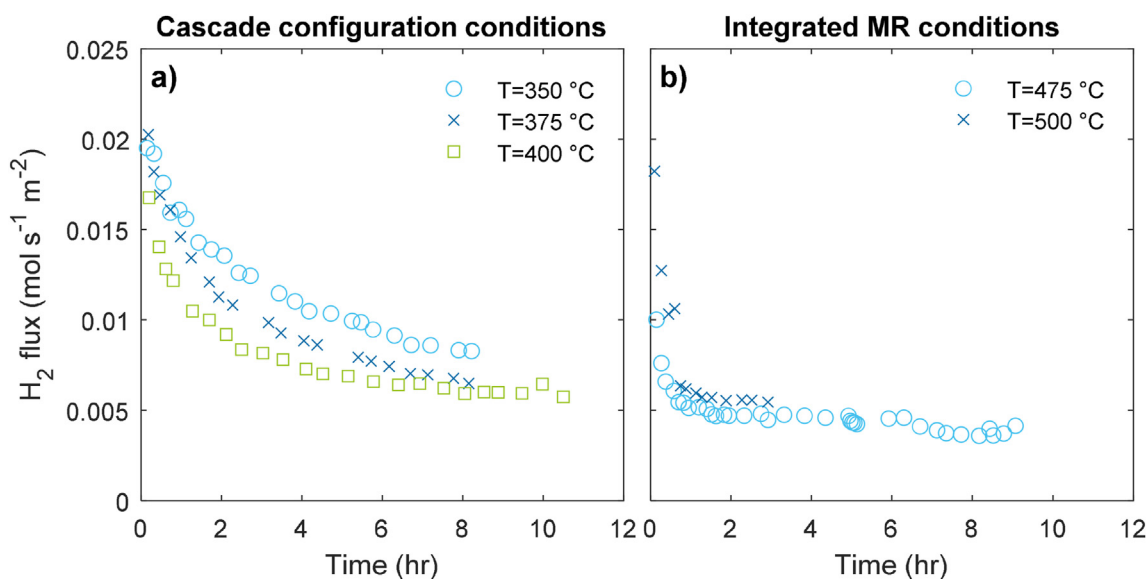


**Fig. 3 – a) H<sub>2</sub> flux of M1 over time in cascade configuration conditions; b) H<sub>2</sub> flux of M1 over time in integrated configuration conditions; details on the experimental conditions can be found in Table 2.**

(which is also in line with results reported by other authors) [15,16,18]. In all the applied conditions, the H<sub>2</sub> flux seems to stabilize after some hours of exposure to the deactivating mixtures. A possible explanation for this is that the multi-step permeation mechanism goes towards a state where dissociative adsorption of H<sub>2</sub> becomes the rate-limiting step, due to the coverage of the membrane surface with carbonaceous species. In this state, the steps of the permeation mechanism that are normally rate-determining, like external mass transfer and bulk diffusion in the PdAg layer, have become much less important. A final observation on Fig. 3b is that the flux during the 475 °C experiment is lower than the flux during the 500 °C experiment. This is not in line with the observed decreasing behaviour of the flux with increased temperature during the experiments in cascade configuration. A possible explanation is that at temperatures above 475 °C surface coverage with carbonaceous species does not increase significantly, meaning that other parameters like external mass transfer or hydrogen diffusivity of PdAg are causing a small difference in flux.

After each permeation step, membrane regeneration was necessary. Other works already reported that regeneration in pure H<sub>2</sub> is in most cases not sufficient, therefore (diluted) air treatments are often applied to recover the original membrane [16,18,20,30]. For the experiments with M1, complete regeneration was achieved by feeding a 1:10 air:N<sub>2</sub> mixture to the membranes, the duration of these regenerations for each cycle can be found in Table 3. If the first regeneration step was not successful, extra regeneration steps were applied until the pure H<sub>2</sub> flux was recovered to the value before the permeation test.

To monitor the quality of the membrane during these permeation-regeneration cycles, two performance indicators are important. The Ideal H<sub>2</sub>/N<sub>2</sub> perm-selectivity is an important parameter to assess the selectivity of the membrane and the pure H<sub>2</sub> flux indicates the permeation activity. To calculate these performance indicators, the flux in pure H<sub>2</sub> and N<sub>2</sub> were measured before and after each cycle at the same temperature as the permeation step and a trans-membrane pressure difference of 2 bar.

The membrane regeneration step was repeated until the H<sub>2</sub> flux from before the experiment was achieved. So, every regeneration was successful in terms of activity. However, when looking at the values of the ideal H<sub>2</sub>/N<sub>2</sub> perm-selectivity in Fig. 4a, significant differences during and between the cycles can be observed. Many of the selectivity values reported in Fig. 4 are indicated with a greater-than sign, in these cases the N<sub>2</sub> permeate flow was too low to be measured (i.e. <0.2 ml min<sup>-1</sup>), and thus the reported values are the minimum perm-selectivity that could be calculated (assuming N<sub>2</sub> flow = 0.2 ml min<sup>-1</sup>).

During the first three permeation-regeneration cycles, N<sub>2</sub> leakage through the membrane could not be measured, meaning that the selectivity remained very high. N<sub>2</sub> leakage and the consequent drop of selectivity was observed during the permeation step of cycle 5. In this cycle the temperature was increased from 350 °C to 475 °C. It is worth mentioning that an increased selectivity is expected at higher temperatures [21]. Leakages may occur through the membranes or through the sealings. Regarding the former mechanism, a possible explanation is the fact that the membrane was

activated and stabilized at 400 °C prior to all experiments. When increasing the temperature above the activation temperature the membrane morphology and therefore the permeation properties might change to some extent, so defects might appear in the PdAg layer.

During the regeneration cycle at 475 °C, the most significant drop of selectivity is observed, caused by an increase of N<sub>2</sub> leakage which can be seen in Fig. 4b. There are different explanations possible for this increase of N<sub>2</sub> leakage: 1) defects in the PdAg layer form as a result of membrane ageing, which is accelerated at higher temperatures, or 2) high temperature air exposure is damaging the membrane, or 3) the sealing is damaged by the applied conditions. Previous research into the effect of air exposure to Pd-alloy surfaces revealed at 500 °C a significant change of the surface morphology, which occasionally also means that defects/holes are opened in the thin PdAg layer [31]. Fig. 4a shows that this phenomenon can take place as well at 475 °C. After increasing the temperature from 475 °C to 500 °C, again an increase of N<sub>2</sub> leakage is observed during the permeation step, even though at higher temperature lower N<sub>2</sub> leakage is expected due to the increase of the gas viscosity. Therefore, it is likely that this increased leakage is a result of membrane defects forming due to the increased temperature. The possibility of leakage through the sealing is of course possible, but this will be ruled out in the next paragraph. Finally, during the regeneration step of cycle 6 at 500 °C, the N<sub>2</sub> leakage of M1 increased even more, most probably as a combination of thermal ageing and damage from air exposure at high temperature or hotspot formation due to combustion of carbon species on the membrane surface.

In order to identify whether the observed N<sub>2</sub> leakage is caused by damage to the sealing or the PdAg layer, the spent M1 membrane was characterized for leakages at 20 °C. The N<sub>2</sub> leakage at 20 °C was compared to the leakage in the last experiment at 500 °C in Fig. 5. At 20 °C the N<sub>2</sub> transport through the membrane defects is much higher since gas viscosity is lower at low temperature. To further evaluate possible leakage from the sealing, the sealings were covered with a silicon resin and N<sub>2</sub> leakage was measured again. As can be seen in Fig. 5, the observed N<sub>2</sub> leakage was nearly equal with and without the added silicon resin cover of the sealings, pointing out that the contribution of the PdAg layer makes up for practically the entire leakage of the membrane. The membrane was then immersed in ethanol to visualize the location(s) of the leakage. It was observed that most of the leakage was coming from one particular spot on the membrane surface. The membrane was then dried, the observed spot of leakage was as well covered with resin and the leakage of the membrane was measured again. From Fig. 5 it is clear that the observed pinhole made up for almost 90% of the entire leakage of the membrane. It is not possible to determine the cause for the formation of such large defect with certainty. However, based on the N<sub>2</sub> leakage extent during the permeation-regeneration tests (Fig. 4) it is likely that air exposure at high temperature enhanced the formation of defects in the PdAg layer (due to the possible hot spots caused by carbon combustion), and there is a progressive membrane deterioration during repeated carbon deposition and removal cycles.

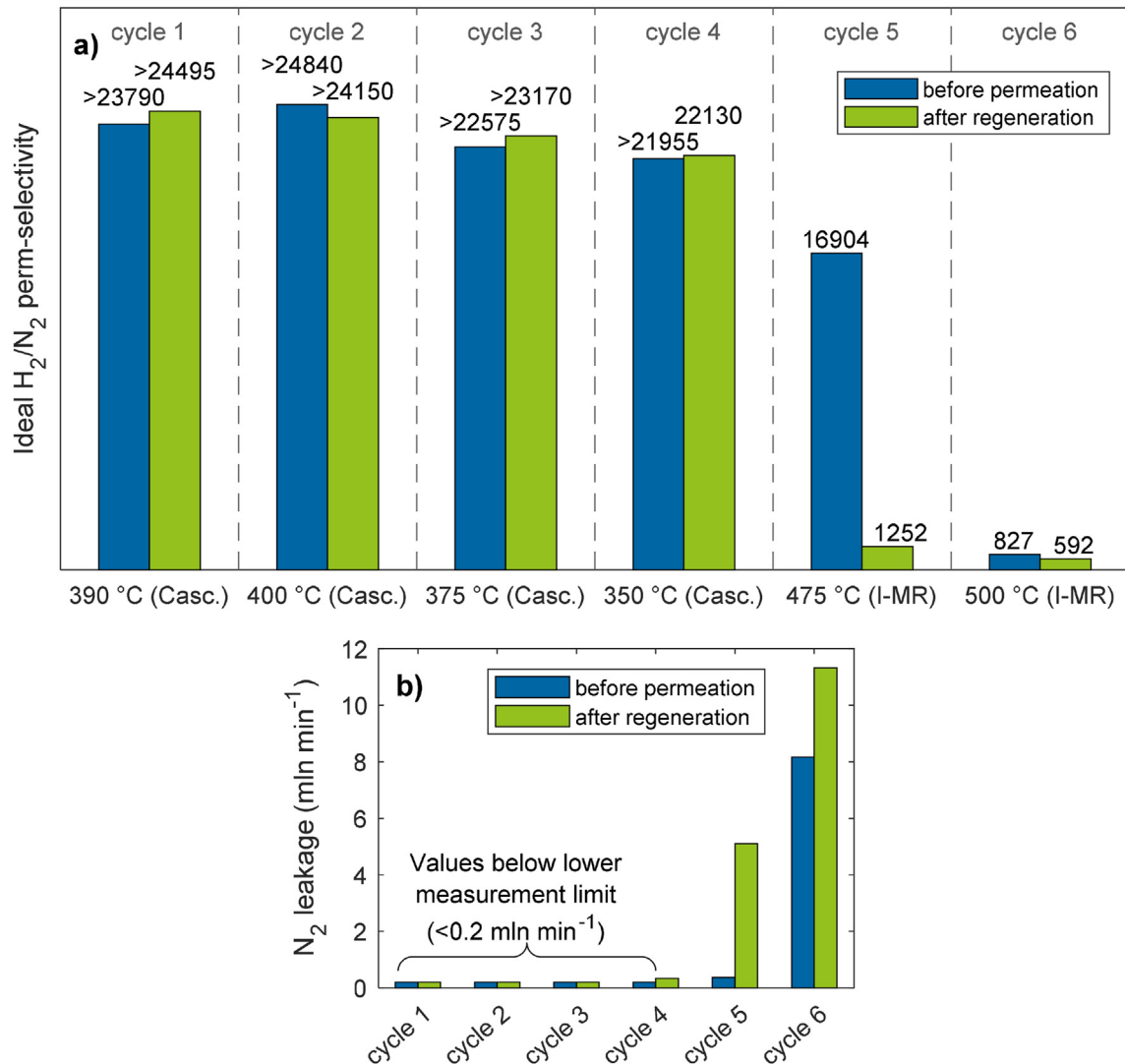


Fig. 4 – a) Ideal  $H_2/N_2$  perm-selectivity of M1 in fresh and regenerated state for each permeation-regeneration cycle and  $N_2$  leakage of M1 in fresh and regenerated state.  $H_2$  and  $N_2$  fluxes were measured at  $\Delta p = 2$  bar in pure  $H_2$  and  $N_2$ .

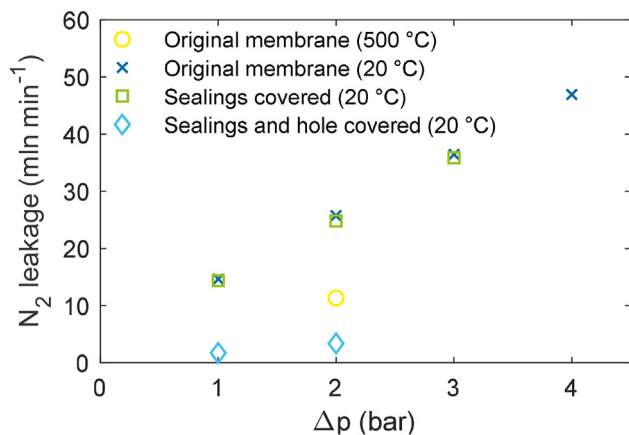
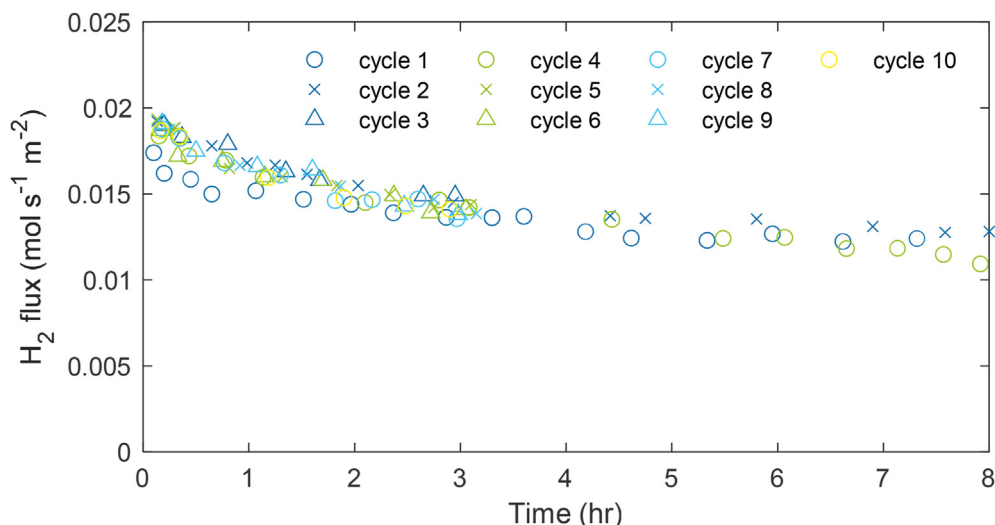


Fig. 5 –  $N_2$  leakage identification by performing  $N_2$  permeation tests on membrane M1 with different parts of the membrane covered using silicon resin

Summarizing the results of membrane M1, the tests have shown that both membrane performance and lifetime are strongly reduced when exposed to propane dehydrogenation and regeneration cycles at high temperature. Therefore, next experiments were focused on evaluation of the membrane performance in the milder cascade configuration process conditions.

#### Repeatability and regeneration (M2)

M2 was repeatedly exposed to permeation-regeneration cycles at 350 °C with cascade configuration conditions. Different regenerations were performed to see their effect on the membrane performance. In Fig. 6, the  $H_2$  flux over time is plotted for each permeation cycle. Quite consistent behaviour can be observed, similar to what was observed for M1 (Fig. 3a). These results demonstrate that the used DS-PdAg membrane deactivates and can be regenerated consistently at 350 °C.



**Fig. 6** –  $H_2$  flux over time of M2 exposed to cascade configuration conditions at 350 °C, 7x 3-h cycle and 3x 8-h cycle.

In the experiments at 350 °C still a significant amount of membrane deactivation was observed. Therefore, an additional test was performed at 300 °C to see if further reduction of temperature can be an effective strategy to improve the performance of the membrane in PDH conditions. In Fig. 7, the  $H_2$  fluxes over time during exposure to cascade configuration conditions at 300 °C and 350 °C, are compared. The results show that operation at 300 °C shows a significantly higher  $H_2$  flux than at 350 °C.

In the experiments performed with M1, it was shown that air exposure enhances the formation of defects in the membrane. Therefore, regeneration tests were focussed on trying to reduce or avoid air exposure to the membranes during regeneration. To assess the different regeneration steps that were applied, the performance indicators were measured like described for membrane M1. So ideal  $H_2/N_2$  perm-selectivity and flux in pure  $H_2$  before and after each cycle are used as performance indicators for selectivity and activity respectively.

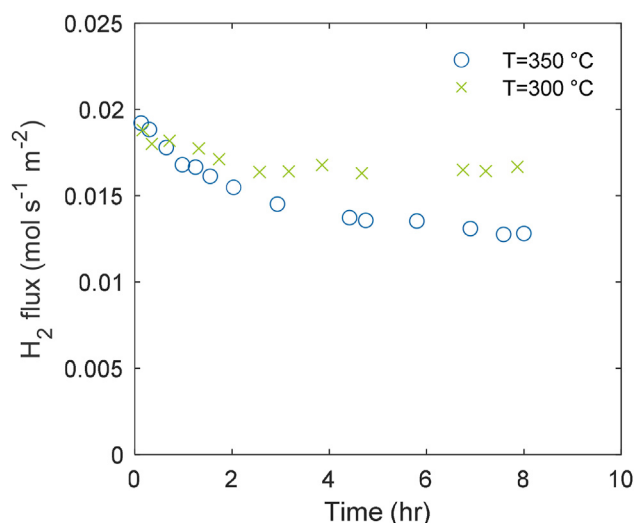


**Fig. 7** –  $H_2$  flux over time of M2 exposed to cascade configuration conditions at 350 °C and 300 °C.

The  $N_2$  permeation flow could not be measured during any of the cycles, since it was below the detection limit of the used flow meters ( $<0.2 \text{ mln min}^{-1}$ ), meaning that the ideal  $H_2/N_2$  perm-selectivity remained above 19,000 at any time. Compared to the results of M1, this was already a significant improvement of the membrane durability. This demonstrates that lowering the temperature of the cycles and optimizing the regeneration conditions results in significant reduction of the membrane degradation.

Due to the significant membrane degradation observed during the cycles with M1, which was mainly attributed to the regeneration step, avoiding the presence of  $O_2$  in the regeneration step would be a possible strategy to improve the lifetime of the membrane. Since a previous investigation into the effect of steam on PdAg membranes showed that  $H_2O$  has a certain surface activity on the surface of a PdAg membrane, it might as well influence surface adsorbed species [32]. To see if

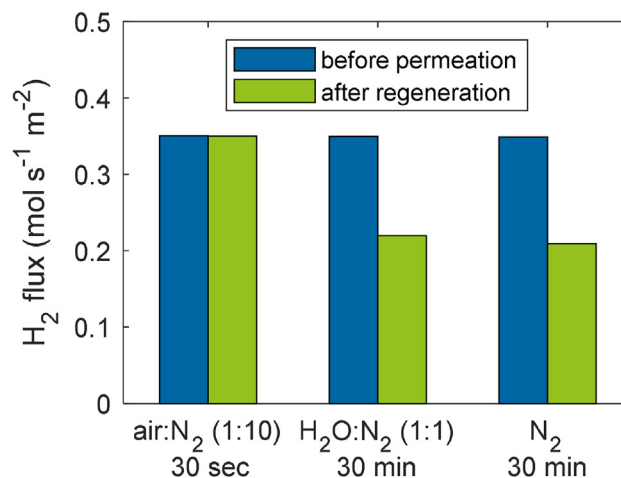


**Fig. 8** – Pure  $H_2$  flux before and after permeation-regeneration cycles, with varied regeneration gas composition. Each regeneration was performed at 1 atm and 350 °C and after a permeation test of 3 h in cascade configuration conditions.



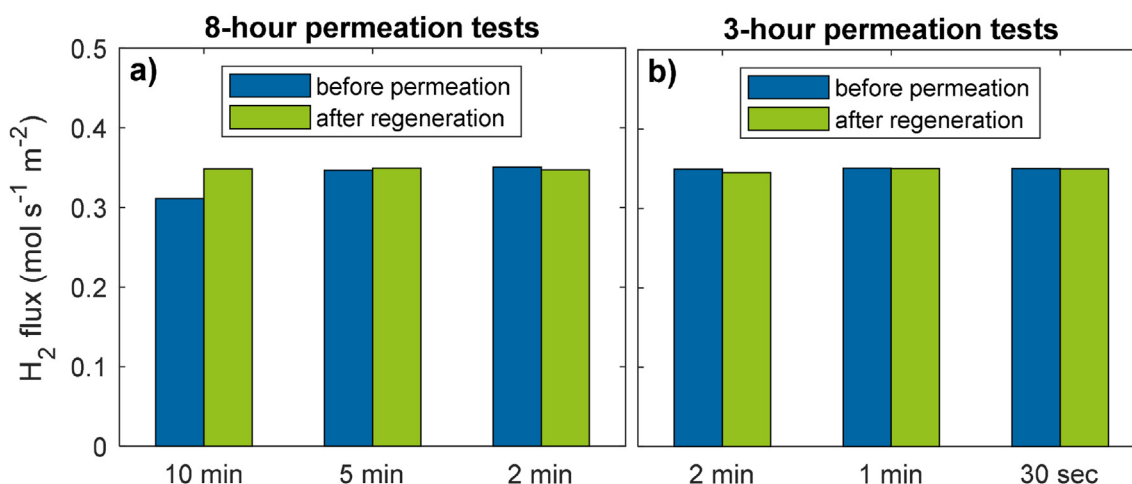


**Fig. 9** – Pure H<sub>2</sub> flux before and after permeation-regeneration cycles, with varied regeneration time. Each regeneration was performed in 1:10 air:N<sub>2</sub> ratio and at 1 atm and 350 °C. Data in a) was obtained after an 8-h permeation test and b) after a 3-h permeation test, both in cascade configuration conditions.

contacting the deactivated membrane with steam had any effect, the membrane in deactivated state was exposed for 30 min to a 1:1H<sub>2</sub>O:N<sub>2</sub> mixture at 350 °C. The experiment was also performed without the addition of H<sub>2</sub>O for comparison. In Fig. 8, the results of these regenerations in H<sub>2</sub>O:N<sub>2</sub> and N<sub>2</sub> are compared to a “default” regeneration procedure of 1:10 air:N<sub>2</sub> for 30 s. The results clearly show that the addition of H<sub>2</sub>O has no regenerative effect. From this we can conclude that the presence of O<sub>2</sub> is necessary to regenerate the surface of the PdAg membrane.

In Fig. 9, the effect of the regeneration time is evaluated. In Fig. 9a, regeneration after 8-h permeation steps is shown. Regeneration is successful for each value of regeneration time (from 2 to 10 min) since H<sub>2</sub> flux reached at least the same level as before the cycle. After the 10 min regeneration even a

higher H<sub>2</sub> flux was observed, probably due to an extra activation effect taking place after the first permeation step. In Fig. 9b the permeation time is decreased to 3 h while regeneration time varies between 30 s–2 min. It is shown that reducing the regeneration time up until 30 s does not affect the full recovery of the membrane activity.

Finally, the dilution ratio of air:N<sub>2</sub> has been decreased from 1:10 to 1:20, and results are reported in Fig. 10. It is shown that an air:N<sub>2</sub> ratio of 1:20 is still successful for regeneration. The results of the varied regeneration conditions show that the regeneration step at lower temperature can be optimized. The exposure time to an O<sub>2</sub> containing mixture can be reduced and also the dilution ratio can be increased without reducing the effectiveness of the regeneration step. However, it must be noted that a short regeneration step will be very sensitive to the properties of the module (i.e. residence time, coke deposited on module walls etc.). Therefore, the optimized the regeneration conditions cannot simply be replicated in a different membrane system.

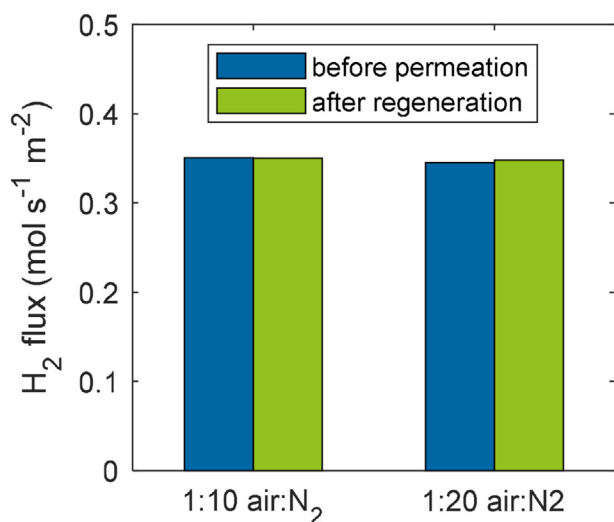


**Fig. 10** – Pure H<sub>2</sub> flux before and after permeation-regeneration cycles, with varied dilution ratio. Each regeneration was performed in at 1 atm and 350 °C, after a 3-h permeation test.

## Conclusions

In this work DS-PdAg membranes have been tested with the objective to evaluate their applicability in the propane dehydrogenation process. Tests were performed in emulated cascade and integrated configurations at higher and lower temperatures. The results show that the performance of the membrane is optimized by operation at the lower temperature of 300 °C. At higher temperature (475 °C and 500 °C), both fast deactivation during exposure to the PDH mixture and fast membrane degradation during regeneration in diluted air atmosphere were observed. This shows that the current DS-PdAg are suitable for the cascade configuration operated at lower temperature (300–350 °C) instead of the integrated one.

Additionally, repeated permeation-regeneration cycles showed that the DS-PdAg membrane could be deactivated and regenerated multiple times, showing consistent performance at 350 °C. The variation of regeneration conditions showed that the

presence of O<sub>2</sub> is necessary to completely regenerate the DS-PdAg membrane after deactivation in PDH conditions. Short and strongly diluted regeneration conditions of 1:20 air:N<sub>2</sub> (1 v% O<sub>2</sub>) for 30 s were found to be sufficient to regenerate a membrane that was exposed to cascade configuration conditions for 3 h.

### Declaration of competing interest

The authors declare that they have no known competing financial interests or personal relationships that could have appeared to influence the work reported in this paper.

### Acknowledgements



This work has received funding from the European Union's Horizon 2020 Research and Innovation Program under grant agreement No 869896 (MACBETH).

### REFERENCES

- [1] Global propylene market - industry trends & forecast report 2028.
- [2] Amghizar I, Vandewalle LA, Van Geem KM, Marin GB. New trends in olefin production. *Engineering* 2017;3(2):171–8. <https://doi.org/10.1016/j.eng.2017.02.006>.
- [3] Farshi A, Shaiyegh F, Burogerdi SH, Dehgan A. FCC process role in propylene demands. *Petrol Sci Technol* 2011;29(9):875–85. <https://doi.org/10.1080/10916460903451985>.
- [4] Wagner da Silva M. Propylene production routes – available ways to improve the profitability of the refining hardware. LinkedIn; 2021 [Online]. Available: <https://www.linkedin.com/pulse/propylene-production-routes-available-ways-improve-da-silva-mba>. [Accessed 17 November 2022].
- [5] Wang G, et al. Recent progress on catalyst supports for propane dehydrogenation. *Curr Nanosci* 2022;18. <https://doi.org/10.2174/1573413718666220616090013>.
- [6] Ricca A, Palma V, Iaquaniello G, Palo E, Salladini A. Highly selective propylene production in a membrane assisted catalytic propane dehydrogenation. *Chem Eng J* 2017;330(August):1119–27. <https://doi.org/10.1016/j.cej.2017.08.064>.
- [7] Kim SJ, et al. Thin hydrogen-selective SAPO-34 zeolite membranes for enhanced conversion and selectivity in propane dehydrogenation membrane reactors. *Chem Mater* 2016;28(12):4397–402. <https://doi.org/10.1021/acs.chemmater.6b01458>.
- [8] Collins JP, et al. Catalytic dehydrogenation of propane in hydrogen permselective membrane reactors. *Ind Eng Chem Res* 1996;35(12):4398–405. <https://doi.org/10.1021/ie960133m>.
- [9] Shelepova EV, Vedyagin AA, Mishakov IV, Noskov AS. Simulation of hydrogen and propylene coproduction in catalytic membrane reactor. *Int J Hydrogen Energy* 2015;40(8):3592–8. <https://doi.org/10.1016/j.ijhydene.2014.09.004>.
- [10] Shelepova EV, Vedyagin AA. Theoretical prediction of the efficiency of hydrogen production via alkane dehydrogenation in catalytic membrane reactor. *Hydro* 2021;2(3):362–76. <https://doi.org/10.3390/hydrogen2030019>.
- [11] Dangwal S, et al. Propane dehydrogenation reaction in a high-pressure zeolite membrane reactor. *Energy Fuel* 2021;35(23):19362–73. <https://doi.org/10.1021/acs.energyfuels.1c02473>.
- [12] Gallucci F, Fernandez E, Corengia P, van Sint Annaland M. Recent advances on membranes and membrane reactors for hydrogen production. *Chem Eng Sci* 2013;92:40–66. <https://doi.org/10.1016/j.ces.2013.01.008>.
- [13] Quicker P, Höllein V, Dittmeyer R. Catalytic dehydrogenation of hydrocarbons in palladium composite membrane reactors. *Catal Today* 2000;56(1–3):21–34. [https://doi.org/10.1016/S0920-5861\(99\)00259-X](https://doi.org/10.1016/S0920-5861(99)00259-X).
- [14] Sheintuch M, Dessau RM. Observations, modeling and optimization of yield, selectivity and activity during dehydrogenation of isobutane and propane in a Pd membrane reactor. *Chem Eng Sci* 1996;51(4):535–47. [https://doi.org/10.1016/0009-2509\(95\)00285-5](https://doi.org/10.1016/0009-2509(95)00285-5).
- [15] Peters TA, Liron O, Tschentscher R, Sheintuch M, Bredesen R. Investigation of Pd-based membranes in propane dehydrogenation (PDH) processes. *Chem Eng J* 2016;305:191–200. <https://doi.org/10.1016/j.cej.2015.09.068>.
- [16] Brencio C, Fontein FWA, Medrano JA, Di Felice L, Arratibel A, Gallucci F. Pd-based membranes performance under hydrocarbon exposure for propane dehydrogenation processes: experimental and modeling. *Int J Hydrogen Energy* 2022;47(21):11369–84. <https://doi.org/10.1016/j.ijhydene.2021.09.252>.
- [17] Abir H, Sheintuch M. Modeling H<sub>2</sub> transport through a Pd or Pd/Ag membrane, and its inhibition by co-adsorbates, from first principles. *J Membr Sci* 2014;466:58–69. <https://doi.org/10.1016/j.memsci.2014.04.028>.
- [18] Jung SH, Kusakabe K, Morooka S, Kim SD. Effects of co-existing hydrocarbons on hydrogen permeation through a palladium membrane. *J Membr Sci* 2000;170(1):53–60. [https://doi.org/10.1016/S0376-7388\(99\)00357-9](https://doi.org/10.1016/S0376-7388(99)00357-9).
- [19] Peters TA, Polfus JM, van Berkel PPF, Bredesen R. Interplay between propylene and H<sub>2</sub>S co-adsorption on the H<sub>2</sub> flux characteristics of Pd-alloy membranes employed in propane dehydrogenation (PDH) processes. *Chem Eng J* 2016;304:134–40. <https://doi.org/10.1016/j.cej.2016.06.065>.
- [20] Montesinos H, Julián I, Herguido J, Menéndez M. Effect of the presence of light hydrocarbon mixtures on hydrogen permeance through Pd-Ag alloyed membranes. *Int J Hydrogen Energy* 2015;40(8):3462–71. <https://doi.org/10.1016/j.ijhydene.2014.11.054>.
- [21] Arratibel A, Pacheco Tanaka A, Laso I, van Sint Annaland M, Gallucci F. Development of Pd-based double-skinned membranes for hydrogen production in fluidized bed membrane reactors. *J Membr Sci* 2018;550(August 2017):536–44. <https://doi.org/10.1016/j.memsci.2017.10.064>.
- [22] Yang Y, et al. Preparation of thin (~2 μm) Pd membranes on ceramic supports with excellent selectivity and attrition resistance. *Int J Hydrogen Energy* 2023;48(2):662–75. <https://doi.org/10.1016/j.ijhydene.2022.10.016>.
- [23] Liu J, et al. Hydrogen permeation and stability in ultra-thin Pd–Ru supported membranes. *Int J Hydrogen Energy* 2020;45(12):7455–67. <https://doi.org/10.1016/j.ijhydene.2019.03.212>.
- [24] Basile A, De Falco M, Centi G, Iaquaniello G. *Membrane reactor engineering*. 2016.
- [25] Brencio C, Di Felice L, Gallucci F. Fluidized bed membrane reactor for the direct dehydrogenation of propane: proof of

- concept. *Membranes* 2022;12(12). <https://doi.org/10.3390/membranes12121211>.
- [26] de Nooijer N, et al. Long-term stability of thin-film Pd-based supported membranes. *Processes* 2019;7(2). <https://doi.org/10.3390/pr7020106>.
- [27] Ali Z. H2SITE to scale membrane reactor breakthrough technology. 6 July 2022. 2022. [Online]. Available: <https://www.h2bulletin.com/h2site-to-scale-membrane-reactor-breakthrough-technology/>. [Accessed 14 November 2022].
- [28] Brencio C, Gough R, de Leeuw den Bouter A, Arratibel A, Di Felice L, Gallucci F. Kinetic model for Pd-based membranes coking/deactivation in propane dehydrogenation processes. *Chem Eng J* 2023;452(P1):139125. <https://doi.org/10.1016/j.cej.2022.139125>.
- [29] Caravella A, Hara S, Drioli E, Barbieri G. Sieverts law pressure exponent for hydrogen permeation through Pd-based membranes: coupled influence of non-ideal diffusion and multicomponent external mass transfer. *Int J Hydrogen Energy* 2013;38(36):16229–44. <https://doi.org/10.1016/j.ijhydene.2013.09.102>.
- [30] Al-Shammary AFY, Caga IT, Winterbottom JM, Tata AY, Harris IR. Palladium-based diffusion membranes as catalysts in ethylene hydrogenation. *J Chem Technol Biotechnol* 1991;52(4):571–85. <https://doi.org/10.1002/jctb.280520414>.
- [31] Roa F, Way JD. The effect of air exposure on palladium-copper composite membranes. *Appl Surf Sci* 2005;240(1–4):85–104. <https://doi.org/10.1016/j.apsusc.2004.06.023>.
- [32] Catalano J, Giacinti Baschetti M, Sarti GC. Influence of water vapor on hydrogen permeation through 2.5  $\mu\text{m}$  Pd-Ag membranes. *Int J Hydrogen Energy* 2011;36(14):8658–73. <https://doi.org/10.1016/j.ijhydene.2011.03.139>.